Journal of Catalysis 266 (2009) 268–278

Contents lists available at ScienceDirect

Journal of Catalysis

journal homepage: www.elsevier.com/locate/jcat

Synthesis, characterization, and catalytic properties of H-Al-YNU-1 and H-Al-MWW with different Si/Al ratios

Weibin Fan [a,*], Shuquan Wei [b], Toshiyuki Yokoi [c], Satoshi Inagaki [d], Junfen Li [a], Jianguo Wang [a], Junko N. Kondo [c], Takashi Tatsumi [c,*]

[a] State Key Laboratory of Coal Conversion, Institute of Coal Chemistry, Chinese Academy of Sciences, 27 South Taoyuan Road, P.O. Box 165, Taiyuan 030001, China
[b] College of Chemistry and Chemical Engineering, Harbin Normal University, Harbin 150025, China
[c] Chemical Resources Laboratory, Tokyo Institute of Technology, Nagatsuta 4259, Midori-ku, Yokohama 226-8503, Japan
[d] Catalysis Laboratory, Division of Materials Science and Chemical Engineering, Graduate School of Engineering, Yokohama National University, Tokiwadai 79-5, Hodogaya-ku, Yokohama 240-8501, Japan

ARTICLE INFO

Article history:
Received 20 March 2009
Revised 15 June 2009
Accepted 17 June 2009
Available online 15 July 2009

Keywords:
H-Al-MWW
H-Al-YNU-1
Zeolite
Postsynthesis
Characterization
Acid catalysis

ABSTRACT

H-Al-MWW with different Si/Al ratios has been synthesized in the presence of hexamethyleneimine by the postsynthesis method with the ion-exchange of Na^+ with NH_4^+ unnecessary. However, irrespective of the framework Si/Al ratio, the as-synthesized Al-MWW lamellar precursor was not transformed into the Al-YNU-1 phase by the method used for preparing Ti-YNU-1 [W. Fan, P. Wu, S. Namaba, T. Tatsumi, Angew. Chem. Int. Ed. 43 (2004) 236]. This may be due to the difficulty in removing hardly oxidized hexamethyleneimine molecules by acid treatment, as shown by TG/DTA measurement results. In combination with ^{13}C CP/MAS NMR spectroscopy, it was indicated that these hardly oxidized hexamethyleneimine molecules might strongly interact with the zeolite framework or be tightly constrained between the layers. Nevertheless such a type of templating molecules could be washed away by acid when piperidine was used as a template. As a result, H-Al-YNU-1 with a pore opening intermediate between those of H-Al-MOR and H-Al-Beta was successfully prepared in the way adopted for preparing Ti-YNU-1. This material showed much higher activity than H-USY, H-Al-MOR, H-Al-Beta, H-Al-MWW, H-Al-ZSM-5, and interlayer-expanded H-Al-MWW through silylation in alkylation of anisole with benzyl alcohol and acylation of anisole with acetic anhydride as a result of its enlarged pore opening connected to supercages and predominant moderately strong Brönsted acid sites. The benefit of the large pore opening of H-Al-YNU-1 was also confirmed by the catalytic results obtained in the Baeyer–Villiger reaction of cyclohexanone with bulkiness corresponding to 12 membered-ring pore openings.

1. Introduction

MWW-type zeolites have a lamellar structure with a 10-membered ring (10-MR) interlayer pore opening connected to a 12-MR supercage ($1.8 \times 1.8 \times 0.72$ nm) and an independent intralayer sinusoidal 10-MR channel [1]. This unique structure gives rise to the material with interesting catalytic properties. It has been shown that the aluminosilicate material MCM-22, namely, Al-MWW, is highly active and selective for benzene alkylation and cracking of *n*-alkanes, making it an FCC octane booster additive specially valuable for the production of reformulated gasolines [2–4]. It is also much more effective than ZSM-5 for producing light oil from Fischer–Tropsch synthesis [5]. The titanosilicate analogue Ti-MWW exhibits quite high activity and selectivity in the epoxidation of linear alkenes in the presence of H_2O_2 aqueous solution [6,7]. Upon delamination of Al-MWW into isolated crystalline sheets, a new zeolitic material of ITQ-2 was obtained with higher activity in the cracking of vacuum oil than zeolite Y as a result of possessing quite large external surface area [8]. Nevertheless, the hydrothermal stability of this material is relatively low because it is rather hydrophilic. In addition, a certain amount of Al-MWW is inevitable to be deteriorated during the delamination process. To overcome this shortage, a new material of Ti-YNU-1 with the structure analogous to MWW-type lamellar precursor has been prepared [9]. Compared to Ti-MWW, Ti-YNU-1 has a significantly expanded interlayer space, and the interlayer pore opening was about 6.7 Å in contrast to 5.2 Å for the Ti-MWW [10]. Thus, Ti-YNU-1 exhibits geometric properties typical of 12-MR zeolites, showing much higher activity and selectivity in the epoxidation of bulky alkenes such as cyclohexene with H_2O_2 than Ti-MWW and TS-1 do [9,10].

Usually, Al-MWW is hydrothermally synthesized from an aluminum-rich synthesis gel (the Si/Al molar ratio <35). Attempts

* Corresponding authors. Fax: +86 351 4041153 (W. Fan), +81 45 924 5282 (T. Tatsumi).
E-mail addresses: fanwb@sxicc.ac.cn (W. Fan), ttatsumi@cat.res.titech.ac.jp (T. Tatsumi).

0021-9517/$ - see front matter © 2009 Elsevier Inc. All rights reserved.
doi:10.1016/j.jcat.2009.06.017

to synthesize high silica Al-MWW from the synthesis gels with low Al contents led to the formation of ZSM-5, ZSM-35, ZSM-51, kenyaite, and/or Nonasil crystalline phases [11–15]. In addition, the high stability of framework Al in Al-MWW against acid and steam made it difficult to obtain high silica Al-MWW by acid treatment and steaming methods [16]. However, high silica Al-MWW would be efficient for catalyzing several types of acidic reactions such as MTO (methanol to olefin), one-step synthesis of dimethyl ether from syngas, and isomerization of 1-butene to isobutene [16,17]. In this context, Al-MWW with a Si/Al molar ratio lower than 500 has been recently synthesized by the postsynthesis method with $NaAlO_2$ as aluminum source [18]. A further decrease in the framework Al content was unsuccessful. Thus, an effort should be made to further increase the framework Si/Al ratio partly because this would be beneficial for an explicit elucidation of preferential occupancy of Al in the crystallographically inequivalent lattice sites and of catalytic reaction mechanism.

Although Ti-YNU-1 was synthesized five years ago by acid washing the postsynthesized high silica Ti-MWW lamellar precursor before calcination [9,10], Al-YNU-1 (or interlayer-expanded Al-MWW) was only very recently attained through postalkoxysilylation of Al-MWW precursor by alkoxysilanes such as diethoxydimethylsilane in HNO_3 acid under reflux conditions [19]. However, this method led to a considerable decrease in the framework Al content. Thus, vapor-phase silylation of Al-MWW lamellar precursor with dichlorodimethylsilane in water was successively developed to decrease Al leaching from the framework [20]. Indeed, it was shown that most of Al species present in the lamellar precursor were still retained after silylation by this method. Nevertheless, a substantial amount of extraframework Al species was present in the Al-YNU-1 samples prepared by both methods. In particular, a significant cleavage of bond connection for expanding the interlayer space occurred during the process of ion exchanging Na^+ with NH_4^+ for the prepared samples, and occasionally resulting in a recovery of Al-YNU-1 to Al-MWW [21]. Therefore, a different route should be developed to avoid the ion-exchange process and the generation of many octahedral Al species in the preparation of H-Al-YNU-1, which would make it stable to act as a unique 12-MR zeolite catalyst. In this paper, we report the synthesis of H-Al-YNU-1 and H-Al-MWW with a Si/Al ratio in the range of 10–∞ without taking a silylation step and their catalytic properties as acid catalysts.

2. Experimental

2.1. Synthesis of samples

Al-containing samples were prepared by the postsynthesis method [22]. First, B-MWW was synthesized with fumed silica (Cab-O-sil, M-7D), boric acid (Wako, 99.5%), piperidine (PI) (TCI, 99%), and distilled water (Wako) in terms of the composition of SiO_2:0.65B_2O_3:1.4PI:19H_2O. The crystallization was carried out at 170 °C for 7–8 days. The as-synthesized solid was calcined and treated with 6 M HNO_3 (Wako, 60–61%) aqueous solution (liquid/solid = 30 mL/g) for more than 20 h at boiling temperature. The highly deboronated sample and aluminum isopropoxide (TCI, 98%) were used as silica and aluminum sources, respectively, to synthesize Al-MWW lamellar precursor with the mixture composed of (0.05–0.15)NH_4OH (Wako, 28%) (or NaOH, Wako, 96%):SiO_2:(0–0.05)Al_2O_3:(1.0–1.4)HMI(PI):(3–20)H_2O (HMI = hexamethyleneimine, TCI, 95%). The resultant mixture was heated to 150–170 °C for 1–7 days under rotating conditions. Finally, the solid product was filtered, washed, dried, and calcined at 550 °C for 10 h to obtain H-Al-MWW. To prepare H-Al-YNU-1, the sample was first treated with 2 M HNO_3 (liquid/solid = 100 mL/g) at boiling temperature before calcination. For comparison, the interlayer-expanded Al-MWW (hereafter designated as Expanded Al-MWW) with the same structure as Al-YNU-1 was prepared by silylation of Al-MWW lamellar precursor with diethoxydimethylsilane (TCI, 98%) in 2 M HNO_3 acid aqueous solution for 20 h at boiling temperature, followed by washing with distilled water, drying, and calcining at 550 °C for 10 h [19]. H-USY (Si/Al = 7), H-Al-Beta (Si/Al = 12.5), and H-Al-MOR (Si/Al = 7.5) were all provided by Tosoh, whereas H-Al-ZSM-5 was obtained from Catalyst Society of Japan (Mobil Corporation, Japan).

2.2. Characterization of samples

The X-ray diffraction (XRD) patterns were recorded on a Rigaku Rint-Ultima III-TK X-ray diffractometer with Cu Kα radiation (40 kV, 20 mA) to identify the crystalline phase and to estimate the crystallinity. Infrared (IR) spectra were measured on a Jasco FTIR 7300 spectrometer with an MCT detector at a resolution of 2 cm^{-1} by accumulating 64 scans. Before pyridine adsorption, the samples were first evacuated at 500 °C for 2 h at about 1 Pa. NH_3 temperature-programmed desorption (NH_3-TPD) was performed on a Multitrack TPD equipment (Japan BEL). ^{27}Al and ^{13}C CP/MAS NMR spectra were measured on a JEOL JNM ECA 400 nuclear magnetic resonance spectrometer at ambient temperature. The chemical shift was referenced to the external standards of $Al(NO_3)_3$ or of tetramethylsilane (TMS). The spinning rate of the rotor was 5.0 kHz. A pulse length of 7 μs and the corresponding magic angle of 90° were applied and about 3000 scans were accumulated with a repetition time of 30 s. The spectra were deconvolved with Gaussian–Lorentzian mixed equation. N_2 adsorption/desorption at −196 °C and cyclohexane adsorption at 25 °C were carried out on Belsorp 28SCA and Belsorp 18SCA instruments, respectively (before measurement, the sample was first pretreated at 250 °C for 3 h under high vacuum conditions). TG/DTA was measured on a MAC Science TG-DTA 2100SA or on a Rigaku Thermal Plus EVO thermal analysis system. The sample weight was about 10 mg. The temperature was ramped to 900 °C at a heating rate of 10 °C/min in an air flow (30 mL/min). The chemical compositions of the samples were determined by an inductively coupled plasma-atomic emission spectrometer (Shimadzu ICPS-8000E).

2.3. Catalytic tests

The liquid-phase alkylation/acylation/Baeyer–Villiger reaction of cyclohexanone was carried out in a round-bottomed flask equipped with a condenser under stirring conditions (see Supplementary material). Temperature was controlled with an oil bath. The detailed reaction conditions for different reactions are shown in the footnotes of tables. The obtained products were analyzed on GC-14B and GC-17B gas chromatographs equipped with flame ionization detectors and 50-m OV-1 and 25-m TC-17 capillary columns, respectively.

3. Results and discussion

3.1. Synthesis of H-Al-MWW

Fig. 1 shows the XRD patterns of highly deboronated B-MWW (denoted as Si-MWW) and the samples synthesized from a synthesis gel having a Si/Al ratio of 15 in the presence of aqueous NH_3. It is clear that Si-MWW material exhibited a typical MWW structure (Fig. 1a). Nevertheless, after crystallization of the mixture of Si-MWW, HMI, aluminum isopropoxide, aqueous NH_3, and distilled water at 170 °C for 2 days, two shoulder peaks appeared at 2θ of

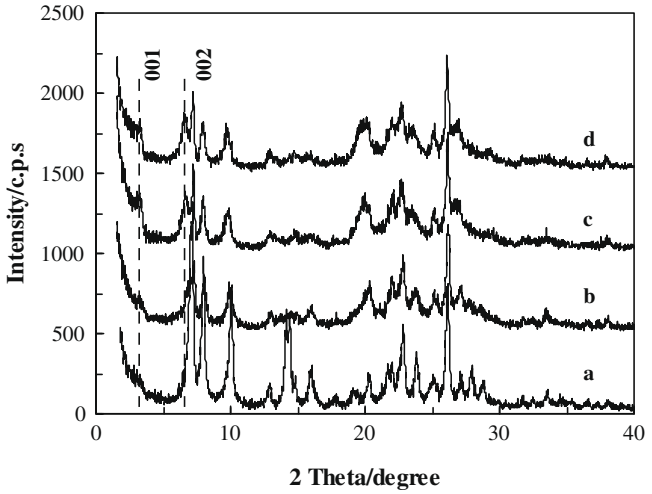

Fig. 1. XRD patterns of the as-synthesized Al-MWW samples postsynthesized at 170 °C for (a) 0 day, (b) 2 days, (c) 4 days, and (d) 7 days in the presence of HMI.

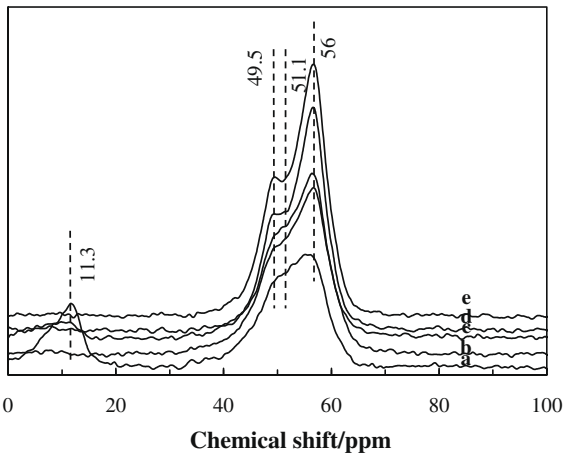

Fig. 3. ^{27}Al MAS NMR spectra of the as-synthesized Al-MWW samples postsynthesized at 170 °C for (a) 1 day, (b) 2 days, (c) 3 days, (d) 5 days, and (e) 7 days with a synthesis gel having a Si/Al ratio of 25 in the presence of HMI.

3.3° and 6.9° in the XRD pattern of the solid product (Fig. 1b), which is assigned to the (001) and (002) diffraction lines of the lamellar MWW precursor [10,23]. These two diffraction lines increased in intensity and became well resolved with increasing crystallization time. When the crystallization time reached 4 days, the product showed a typical XRD pattern of the lamellar MWW precursor (Fig. 1c), confirming the successful transformation of 3D MWW structure into the lamellar structure. A further increase in the crystallization time from 4 to 7 days did not strongly affect the structure of the solid product (Fig. 1d).

ICP measurement showed that the Si/Al ratio of the product decreased to 14.2, being similar to that of the synthesis gel, with increasing crystallization time up to 7 days. The OH-region of IR spectrum of the calcined sample showed a very intense band at 3613 cm^{-1} in addition to the silanol bands at 3745 and 3730 cm^{-1} (Fig. 2), which is characteristic of bridging Si–OH–Al groups and evidences the incorporation of Al in the framework. Four peaks were observed in the ^{27}Al MAS NMR spectra of the samples obtained at different crystallization times (Fig. 3). The signal around 11.3 ppm is due to penta-coordinated Al species, whereas the other three signals at about 49.5, 51.1, and 56.0 ppm are attributed to tetrahedral Al species located at crystallographically inequivalent lattice sites [18,24]. For the sample crystallized at 170 °C for 1 day, the signal at 11.3 ppm was very intense, indicating that a large amount of Al species were not truly inserted into the lattice but tethered on the solid. With crystallization going on, these Al species were progressively incorporated into the framework, as verified by the increase in the intensity of the signals assigned to tetrahedral Al species at the expense of the peak due to penta-coordinated ones. The complete disappearance of penta-coordinated Al species demonstrates that all Al species were incorporated into the framework when the crystallization was carried out at 170 °C for 7 days.

Two intense desorption peaks around 166 and 326 °C were observed in the NH_3-TPD profile of H-Al-MWW prepared by the postsynthesis method (curve c in Fig. 4). This is consistent with that observed with the H-Al-MWW attained by the hydrothermal synthesis method except that the peak corresponding to weak acid sites shifted to 186 °C for the hydrothermally synthesized sample (not shown here) [25]. A deep deboronation of B-MWW before being used as silica source caused generation of a large number of defective sites or silanol groups [9,10], thus leading to formation of much more weak acid sites in the post-prepared sample than in the hydrothermally prepared one [24]. Nevertheless, the amount and acid strength of strong acid sites (Si–OH–Al species) were similar for both the samples. It was found that the amount of the strong acid sites was closely related to the Al content in the sam-

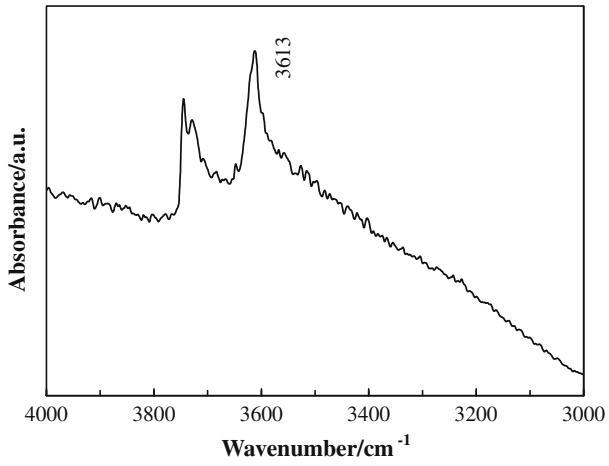

Fig. 2. OH-region of IR spectrum of the calcined Al-MWW sample postsynthesized from a synthesis gel having a Si/Al ratio of 25 in the presence of HMI.

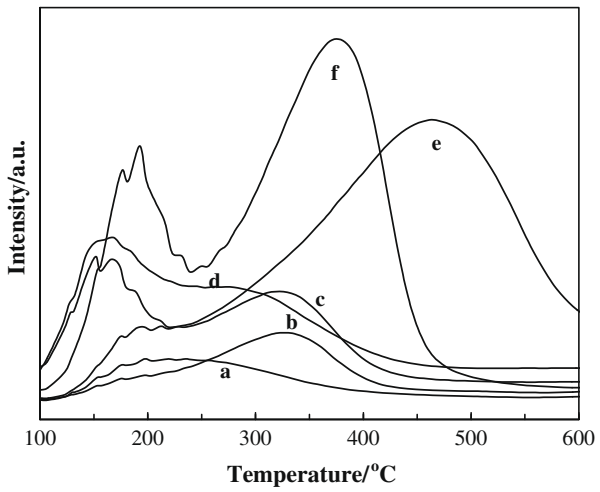

Fig. 4. NH_3-TPD profiles of various zeolites: (a) H-USY, (b) H-Al-YNU-1, (c) H-Al-MWW, (d) H-Al-Beta, (e) H-Al-MOR, and (f) H-Al-ZSM-5.

ple, in agreement with complete insertion of Al in the zeolite framework.

Fig. 5 shows the effect of the amount of NH_3 in the synthesis gel having a Si/Al ratio of 15 on the crystallization. Clearly, a pure MWW-type lamellar precursor was obtained when the NH_3/SiO_2 molar ratio was 0.15 or less (curves a and b). An increase in the NH_3/SiO_2 ratio to 0.2 or more led to the formation of an unknown lamellar phase (curves c and d). When NaOH, instead of aqueous NH_3, was used as alkali, 3D Si-MWW was transformed into the Al-MWW lamellar precursor at a much higher rate for the synthesis gel with a Na/Si ratio of 0.05, although the formation of an impurity material characterized by a diffraction line at 2θ of 4.5° was also found (curve b in Fig. 6). Nevertheless, this transformation became hard to observe with increasing NaOH content in the synthesis gel. This is probably a result of transformation of Si-MWW crystals into the impurity crystalline materials, as indicated by the diffraction lines at 2θ of 4.5°, 9.6°, 22.4°, and 24.7° (curve d in Fig. 6).

Fig. 7 shows the XRD patterns of the samples postsynthesized from synthesis gels having a Si/Al ratio in the range of 15–2000

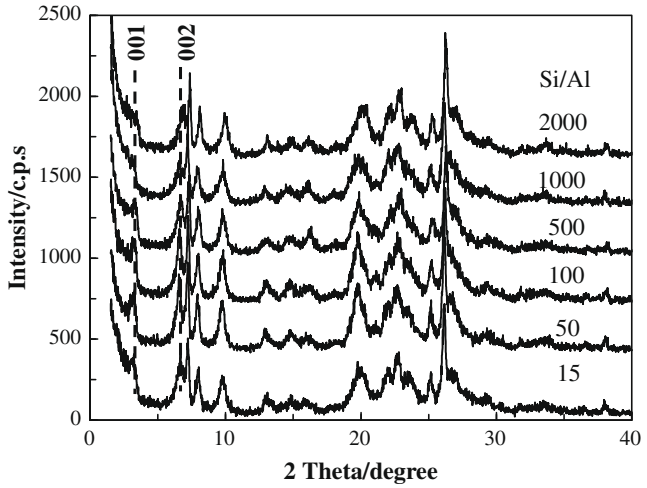

Fig. 7. XRD patterns of the as-synthesized Al-MWW samples postsynthesized with synthesis gels having different Si/Al ratios in the presence of NH_4OH and HMI.

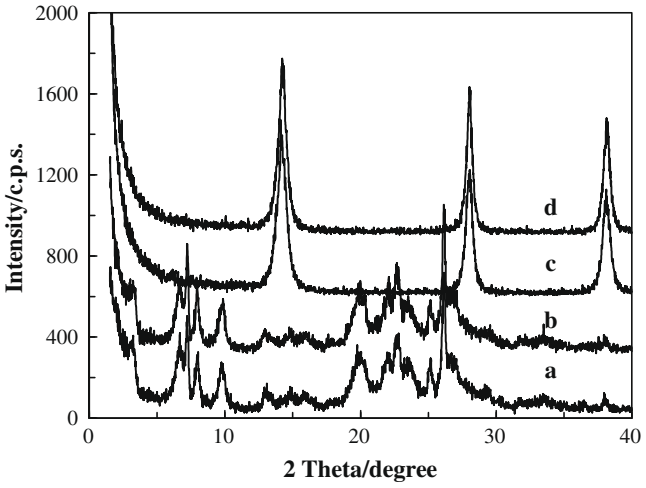

Fig. 5. XRD patterns of the as-synthesized Al-MWW samples postsynthesized with a synthesis gel having a Si/Al ratio of 15 and an NH_3/SiO_2 ratio of (a) 0.1, (b) 0.15, (c) 0.20, and (d) 0.25.

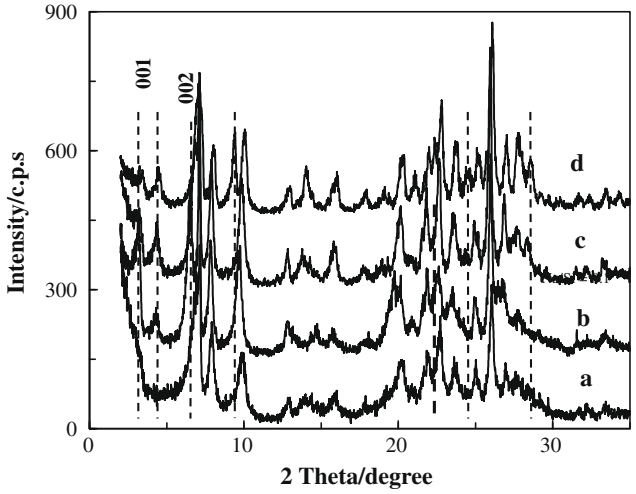

Fig. 6. XRD patterns of the as-synthesized Al-MWW samples postsynthesized at 170 °C for 2 days with a synthesis gel having a Si/Al ratio of 20 and a Na^+/SiO_2 ratio of (a) 0, (b) 0.05, (c) 0.075, and (d) 0.1 in the presence of HMI.

in the presence of aqueous NH_3. Evidently, all samples had the MWW-type lamellar precursor structure, indicting that H-Al-MWW with different Si/Al ratios can be directly obtained in the absence of alkali cations such as Na^+ by the postsynthesis method. In contrast, an ion-exchange process is necessary for the hydrothermally synthesized and postsynthesized samples crystallized in the presence of NaOH or $NaAlO_2$ [18]. In addition, compared to the reported result [18], the Si/Al ratio in H-Al-MWW was considerably increased, as evidenced by the structural conversion of Si-MWW to the Al-MWW lamellar precursor regardless of the Al content in the synthesis gel [18,22]. This increase is probably due to the absence of NaOH in the crystallized mixture. As is shown in Fig. 6, addition of NaOH to the synthesis gel greatly accelerated the transformation of Si-MWW into the lamellar precursor, but it was accompanied by the formation of impurity materials, showing that pure Al-MWW lamellar precursor was difficult to be synthesized by the postsynthesis method in the presence of NaOH. The structure of the formed impurity material depends on the Al content in the synthesis gel. When the synthesis gel with a Si/Al ratio of 61.9 was crystallized at 175 °C for 3 days, the Nonasil phase was formed as an impurity material (Fig. 3 in Ref. [18]), and its amount increases with increasing crystallization time at the expense of the MWW material.

3.2. Synthesis of H-YNU-1

It has been shown that Ti-YNU-1 has the structure analogous to MWW lamellar precursor with an expanded (12-MR in contrast to 10-MR for Ti-MWW) pore opening between layers [9,10,26], showing high activity in the epoxidation of bulky alkenes such as cyclohexene with H_2O_2 as a result of the increase in steric accessibility [9,10,26]. It was supposed that Ti-YNU-1 was constructed through pillaring the crystalline MWW sheets by silica ions during the acid-treatment process [26]. Al-YNU-1 has the same structure as Ti-YNU-1, and was recently prepared by intercalating monomeric silylating agent of diethoxydimethylsilane or dichlorodimethylsilane in the interlayers of as-synthesized Al-MWW lamellar precursors [19,20]. However, the ion-exchange of Na^+ with NH_4^+ was needed for preparing H-Al-YNU-1, as a consequence, leading to a significant breaking of the Al-YNU-1 structure, and occasionally, a recovery of Al-YNU-1 to Al-MWW [21]. Thus, Al-YNU-1 was prepared here with PI as a templating molecule and NH_4^+ or PI^+ as a counter-cation by using the method reported for preparing Ti-YNU-1 [9].

Fig. 8 shows the XRD patterns of the as-synthesized, acid-treated and further calcined samples synthesized by the postsynthesis method in the presence of aqueous NH_3 and PI or HMI. Both of the as-synthesized samples exhibited an XRD pattern typical of the MWW lamellar precursor. However, after acid treatment and further calcination, the (001) and (002) diffraction lines were still clearly visible for the sample synthesized in the presence of PI (designated as Al-MWW-PI) (Fig. 8A), whereas the (002) diffraction line shifted to a high 2θ position, and merged into the (100) line [23] in the case of the sample synthesized with HMI (designated as Al-MWW-HMI) (Fig. 8B), as is the case with direct calcination of the as-synthesized lamellar precursor. This shows that with PI used as a templating molecule, H-Al-YNU-1 can be synthesized by the same method as that used for preparing Ti-YNU-1 [9,10], while it cannot be obtained in the same way when HMI was used.

Fig. 9 displays the cyclohexane adsorption isotherms obtained on various zeolites. Clearly, H-Al-MWW hardly adsorbed cyclohexane due to its 10-MR pore openings, which limited the diffusion of cyclohexane molecules into channels. In contrast, being a 12-MR zeolite, H-Al-YNU-1 had a pore opening larger than the dynamic diameter of cyclohexane molecules, and hence, showing an obvious adsorption of cyclohexane. The adsorption rate and adsorption amount increased in the sequence of H-Al-MOR < H-Al-YNU-1 < H-Al-Beta < H-USY. This is in agreement with the pore openings and pore volumes of these zeolites and with the catalytic results for epoxidation of cyclohexene over different titanosilicates [9].

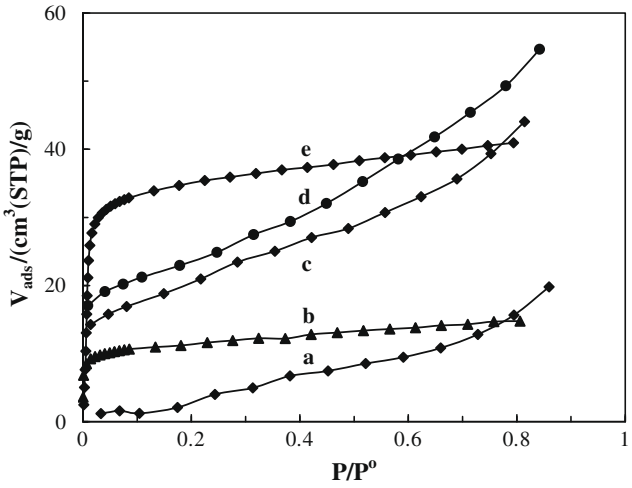

Fig. 9. Cyclohexane adsorption isotherms of various zeolites at 25 °C, (a) H-Al-MWW, (b) H-Al-MOR, (c) H-Al-YNU-1, (d) H-Al-Beta, and (e) H-USY.

As was reported in a previous paper [10], one of the prerequisite conditions for the synthesis of Ti-YNU-1 without taking a silylation step is that most of the templating molecules present in the as-synthesized lamellar precursor could be removed by acid treatment. Such a process would generate a lot of stacking faults between layers [9,10] and might concomitantly produce a small amount of silica "debris" from the framework, which possibly constructs monomeric silica puncheons between the crystalline MWW sheets, resulting in the formation of expanded layer structure of Ti-YNU-1 [20,26].

The TG/DTA results of hydrothermally synthesized Al-MWW lamellar precursor (Si/Al = 20) in the presence of HMI and successively acid-treated sample are shown in Fig. 10. The weight loss below 100 °C is due to desorption of physically adsorbed water, whereas that occurred in the range of 180–240 °C may be assigned to desorption of physically adsorbed and some loosely occluded

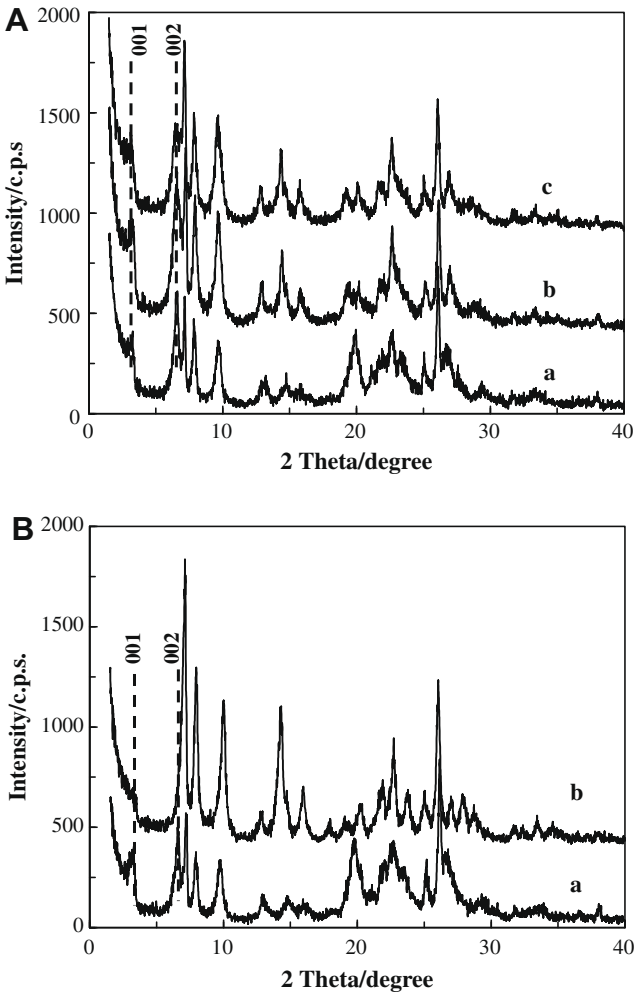

Fig. 8. XRD patterns of (A) (a) postsynthesized Al-MWW-PI lamellar precursor (Si/Al ratio in the synthesis gel was 25), (b) acid-treated sample, and (c) further calcined sample, and (B) (a) postsynthesized Al-MWW-HMI lamellar precursor (Si/Al ratio in the synthesis gel was 50), (b) acid-treated and further calcined sample.

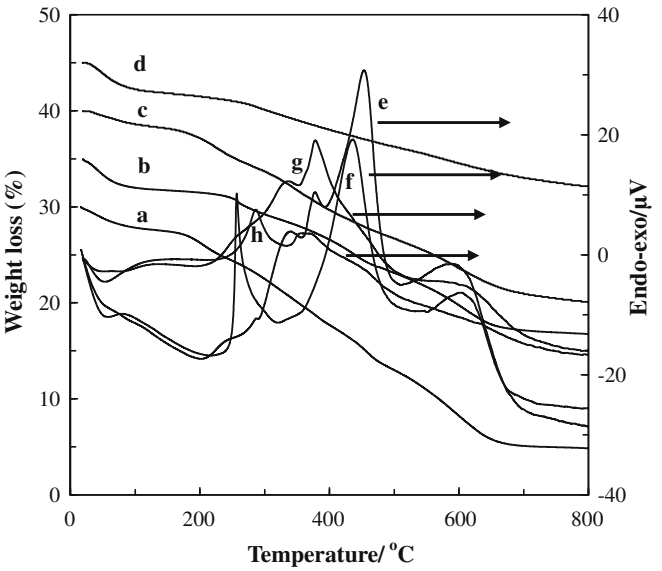

Fig. 10. TG/DTA profiles of the Al-MWW-HMI samples hydrothermally synthesized (a, b, e, and f) with a synthesis gel with a Si/Al ratio of 20 and postsynthesized (c, d, g, and h) with a synthesis gel with a Si/Al ratio of 140: (a, c, e, and g) as-synthesized lamellar precursor; (b, d, f, and h) acid-treated sample.

HMI molecules, as supported by the fact that such a weight loss was not observed for the acid-treated sample because these HMI molecules could be easily washed away by acid. As for the weight loss at the temperature >240 °C, it is mainly attributed to combustion of tightly occluded HMI molecules, as evidenced by the presence of intense exothermic peaks in the corresponding region of the DTA curve. A total weight loss of 21.9% was observed in the range of 180–700 °C for the as-synthesized sample in contrast to 14.2% for the acid-treated one. This shows that about 35% of the HMI molecules present in the as-synthesized lamellar precursor could be removed by the acid treatment.

In the case of Al-MWW-HMI postsynthesized from a synthesis gel having a Si/Al ratio of 140, although the weight loss ascribed to desorption of water was similar to that occurred in the hydrothermally synthesized sample, more than 40% of the HMI molecules present in the as-synthesized sample could be removed by acid washing. Nevertheless, this value is much smaller than that (about 70–80%) observed in the preparation of Ti-YNU-1 [10]. This difference might partially arise from the organic amines used. The Ti-MWW lamellar precursor used for preparing Ti-YNU-1 was synthesized with PI [9], which has a smaller molecular size than HMI, perhaps being easier to be removed by acid treatment.

This could also be the case for the synthesis of H-Al-YNU-1. To confirm this assumption, we treated the Al-MWW-PI lamellar precursor postsynthesized from a synthesis gel having a Si/Al ratio of 25 with acid, and indeed found that the weight loss of the acid-treated sample at the temperature higher than 160 °C was only about 43% of that of the as-synthesized precursor (Fig. 11), showing that about 57% of occluded PI molecules in the as-synthesized precursor could be washed away by acid at boiling temperature. However, an endothermic peak around 227 °C clearly appeared in the DTA curve of the as-synthesized precursor (curve c). This implies that the weight loss due to desorption of occluded water cannot be excluded. If the weight loss between 200 and 700 °C was used to estimate the amount of PI molecules present in the sample according to the suggestions of Liu et al. [18] and Lawton et al. [27], about 55% of the PI molecules in the lamellar precursor could be washed away by acid. This shows that the amount of the PI molecules removed by the acid treatment was indeed larger than that of removed HMI but still much smaller than that observed in the preparation of Ti-YNU-1 from the Ti-MWW-PI lamellar precursor [10]. Nevertheless, the H-Al-YNU-1 could be prepared by acid treating the as-synthesized Al-MWW-PI precursor and following calcination.

It has also been shown that a Si/Ti ratio higher than 80 in the synthesis gel of Ti-MWW lamellar precursor is necessary for the successful preparation of Ti-YNU-1, and that the larger the Si/Ti ratio in the gel is, the better the formed YNU-1 structure is [9,10]. However, the Al-MWW-HMI lamellar precursor postsynthesized from a synthesis gel having a Si/Al ratio as high as 140 could not be converted into the Al-YNU-1 material through acid treatment and successive calcination (Fig. 12); in contrast, Al-YNU-1 could be prepared by the same method from the Al-MWW-PI lamellar precursor synthesized from a synthesis gel with a Si/Al ratio of 25 (Fig. 8A). Therefore, in order to understand well the mechanism of formation of H-Al-YNU-1, we must pay more attention to the location and effect of the PI and HMI molecules on the structure.

3.3. Location of templating molecules (HMI or PI)

When Figs. 10 and 11 are compared, it can be seen that the exothermic peaks around 435 and 593 °C present in the DTA curve of postsynthesized Al-MWW-PI lamellar precursor nearly disappeared after acid treatment at boiling temperature, while these two peaks were still clearly observed in the DTA curve of acid-treated postsynthesized Al-MWW-HMI sample although their intensities decreased compared to those of the as-synthesized lamellar precursor (Fig. 13). This also held true for the hydrothermally synthesized sample (Fig. 10). The amount of HMI removed by the acid treatment was highly dependent on the Si/Al ratio for the postsynthesized lamellar precursor, and the lower the Si/Al ratio was, the smaller the relative amount of removed HMI was. About 25% of the HMI molecules present in the Al-MWW-HMI lamellar precursor postsynthesized from the synthesis gel having a Si/Al ratio of 20 were removed by the acid treatment (Fig. 13) in contrast to 40% observed with the sample postsynthesized with a synthesis gel with a Si/Al ratio of 140 (Fig. 10). This perhaps results from the presence of more protonated HMI molecules in the sample with a low Si/Al ratio, as incorporation of more Al in the framework would create more negative charges in zeolite framework.

Generally, it is believed that the removal of PI or HMI molecules sited at the interlayer space occurs at the temperature below 400 °C, while the oxidation of those in the intralayer 10-MR sinusoidal channels occurs at the temperature >400 °C. If this were true, the amine in the sinusoidal channels should have been re-

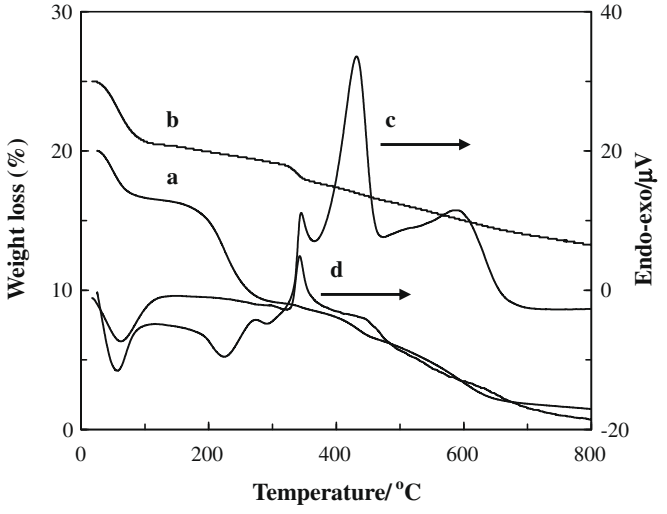

Fig. 11. TG/DTA profiles of the Al-MWW-PI postsynthesized with a synthesis gel having a Si/Al ratio of 25: (a and c) as-synthesized lamellar precursor; (b and d) acid-treated sample.

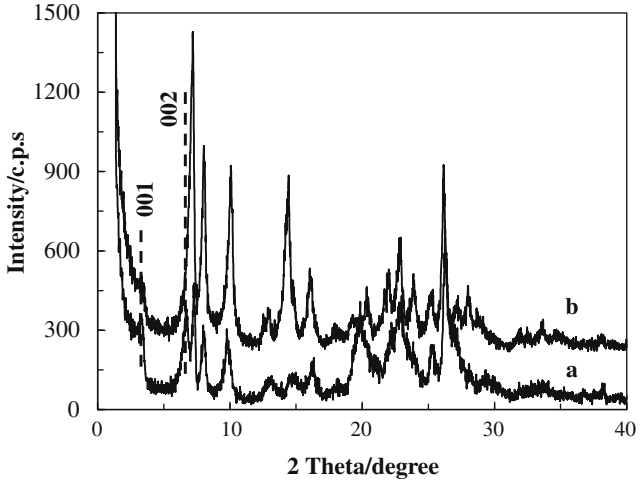

Fig. 12. XRD patterns of the Al-MWW-HMI postsynthesized with a synthesis gel having a Si/Al ratio of 140 (a) as-synthesized lamellar precursor and (b) acid treated and further calcined sample.

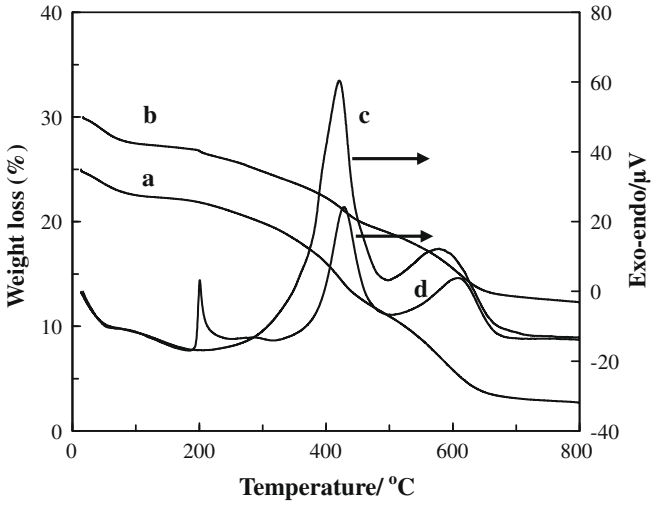

Fig. 13. TG/DTA profiles of the Al-MWW-HMI postsynthesized with a synthesis gel having a Si/Al ratio of 20: (a and c) as-synthesized lamellar precursor; (b and d) acid-treated sample.

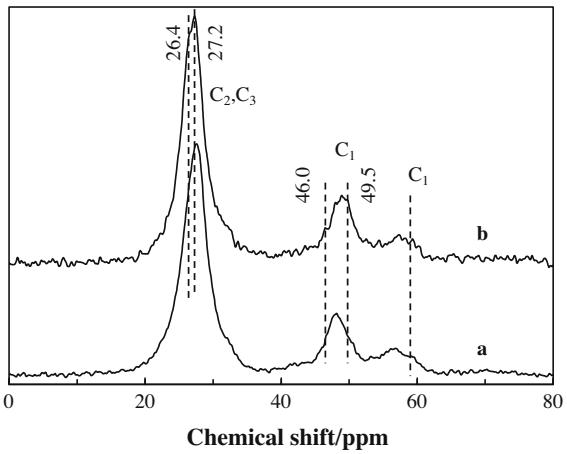

Fig. 14. ^{13}C CP/MAS NMR spectra of hydrothermally synthesized (a) and postsynthesized (b) Al-MWW-HMI lamellar precursors.

moved by the acid treatment. However, this is not in agreement with the rigid intralayer 10-MR pore-opening (≈4.1 × 5.1 Å), which would restrain HMI or PI molecules from entering into the sinusoidal channels during the structural conversion of 3D Si-MWW to Al-MWW lamellar precursor unless decomposition of these two types of templating molecules occurred and/or the zeolitic structure was broken and then rebuilt around them. In addition, it cannot be expected that removal of the HMI or PI molecules located at the intralayer voids would have strong influences on the structure between layers because the intralayer 10-MR sinusoidal channel and supercages are separated by double six-membered rings, prohibiting these molecules from moving to the interlayer void space.

Because it is very difficult to hydrothermally synthesize pure Al-MWW lamellar precursor with PI, here we used the Al-MWW-HMI lamellar precursor as an example to investigate the location of HMI molecules in the hydrothermally synthesized and postsynthesized samples. Figs. 10 and 13 show that the two samples synthesized with the synthesis gels having the same Si/Al ratio of 20 displayed similar TG and DTA profiles except that the hydrothermally synthesized sample showed a larger weight loss (1.4%) than the postsynthesized sample did (0.2%) in the region of 150–200 °C, and that the exothermic peak at about 456 °C for the hydrothermally synthesized sample shifted to 424 °C for the postsynthesized one. A continuous weight loss of 16.9% was observed in the range of 200–700 °C for the postsynthesized Al-MWW-HMI lamellar precursor with a Si/Al ratio of 140. A decrease in the Si/Al ratio of the postsynthesized Al-MWW-HMI precursor to 20 led to a weight loss of 18.9% in the same region (Fig. 13), which is similar to that (19.2%) of the sample hydrothermally synthesized from the synthesis gel having the same Si/Al ratio (Fig. 10). This shows that the postsynthesized Al-MWW-HMI lamellar precursor contained nearly the same amount of HMI molecules as the hydrothermally synthesized one when the Si/Al ratios of both the samples were the same. Since both the precursors are highly crystalline, they would have a similar pore volume. Thus, most of the void space in the framework, including both interlayer space and intralayer 10-MR sinusoidal channels, would be occupied by HMI molecules for both the precursors.

To support this inference, ^{13}C CP/MAS NMR spectra of the hydrothermally synthesized and postsynthesized Al-MWW-HMI lamellar precursors were measured. Fig. 14 shows that the ^{13}C CP/MAS NMR spectrum of the postsynthesized sample was nearly the same as that of the hydrothermally synthesized one; both the samples exhibited three signals around 57, 48, and 27 ppm, which are attributed to C_1, C_1, and overlapped C_2/C_3 carbon resonances of HMI molecules, respectively [27,28]. In agreement with the result reported by Lawton et al. [27,28], the peak area ratio of these three signals was 4.6:1:0.7 for the hydrothermally synthesized sample. It has been suggested that the appearance of two C_1 signals is due to HMI molecules residing in the two different environments, viz. interlayer void space and intralayer sinusoidal channels [27,28]. Nevertheless, subtle but distinct differences were found between the postsynthesized and hydrothermally synthesized samples: (1) a shoulder signal at 26.4 ppm present in the spectrum of the postsynthesized sample was absent in that of the hydrothermally synthesized sample; (2) a much broader signal was observed around 48 ppm for the postsynthesized sample than for the hydrothermally synthesized one, indicating that it was probably an overlapping signal consisting of peaks spanning a range from 46 to 49.5 ppm. It was reported that the carbon signals of protonated HMI shifted to the higher field, compared to those of neutral HMI molecules [27]. If both the neutral and protonated HMI molecules were present in the as-synthesized sample, overlapped C_1 resonances would appear in the region of 45–49 ppm. Thus, the broad peak around 48 ppm suggests that a part of templating molecules present in the postsynthesized lamellar precursor were protonated to balance framework negative charges originating from the incorporation of Al^{3+}. Such would be the case since the postsynthesis system is free of alkali cations. In addition, it was found that the peak area ratio of the three signals of the postsynthesized lamellar precursor was 6:1:0.5, giving an area ratio of the C_2/C_3 signals to the C_1 was 4 in contrast to 2.7 for the hydrothermally synthesized sample. The large deviation from 2 suggests that decomposition of a part of HMI molecules possibly occurred during the crystallization process in the postsynthesis system [27,28] although the signals due to the species formed from the partial decomposition of HMI molecules were not observed. The reason for unobserving the signals attributed to the partially decomposed HMI species was not clear for the moment. It might be due to the overlap of these signals with the C_2/C_3 and/or C_1 signals. This is supported by the shift of the DTA peak attributed to combustion of occluded HMI molecules from 456 °C for the hydrothermally synthesized sample to 424 °C for the postsynthesized one (Figs. 10 and 13). This could account for diffusion of templating molecules into distorted 10-MR interlayer void space and intralayer sinusoidal channels from mother liquid. The interlayer space would be progressively expanded by accommodating more HMI molecules.

Fig. 15 displays the ^{13}C CP/MAS NMR spectra of hydrothermally synthesized B-MWW-PI and postsynthesized Al-MWW-PI lamellar precursors. Both spectra showed mainly three signals; the two peaks at 23.8 and 58.9 ppm of the B-MWW-PI lamellar precursor shifted to 23.2 and 58.2 ppm for the postsynthesized Al-MWW-PI lamellar precursor, respectively. This is probably due to the much stronger protonation of PI molecules to balance framework negative charges in the Al-MWW-PI lamellar precursor than in the B-MWW-PI precursor as a result of Al–O bond strength being significantly higher than B–O bond strength. Although the area ratio of the three signals of the B-MWW-PI precursor was 2.25:1:0.34 in contrast to 1.86:1:0.15 for the postsynthesized Al-MWW-PI lamellar precursor, the peak area ratios (1.68 vs. 1.62) of the C_2/C_3 signals to the C_1 were similar for both the samples, being close to 1.5. This shows that the incorporated PI was mostly intact except for protonation, being different from HMI probably because of its small molecular size. It was found that Al-MWW-PI lamellar precursor could be postsynthesized at 170 °C for 1 h (not shown here), whereas the synthesis of Al-MWW-HMI lamellar precursor at 170 °C in the postsynthesis system needed 4 days (Fig. 1).

For both the hydrothermally synthesized and the postsynthesized Al-MWW-HMI lamellar precursors, the DTA profiles in the high temperature region were almost unchanged after the acid treatment, although the peaks were slightly shifted in position and decreased in intensity. Nevertheless, a remarkable difference was observed in the DTA profiles between 200 and 400 °C (Figs. 10 and 13); the two peaks at 340 and 380 °C drastically decreased in intensity, and even disappeared after the acid treatment, while a new exothermic peak at 257 °C for the hydrothermally synthesized sample or an one at 200 °C for the postsynthesized precursor was observed. In the TG curve of the hydrothermally synthesized Al-MWW-HMI lamellar precursor, there were three weight-loss regions in the range from 150 to 700 °C, viz. 150–400, 400–469, and 469–700 °C. From the viewpoint of geometric structure of MWW-type materials, it is believable that the PI or HMI molecules located in the intralayer 10-MR sinusoidal channels are more difficult to be removed by acid treatment than the PI or HMI molecules in the interlayer void space. However, after the acid treatment, the weight losses in the above three regions were about 52.7%, 77.4%, and 51.0% of those observed with the as-synthesized sample, respectively. This suggests that the HMI molecules oxidized at high temperature (469–700 °C) might also be located at the void space between layers. This held true for the postsynthesized Al-MWW-HMI lamellar precursor. This is possibly associated with the HMI molecules interacting with zeolite framework and tightly constrained in the interlayer space, as supported by the increase in the intensity of exothermic peaks with increasing framework Al content (Figs. 10 and 13). The appearance of a new exothermic peak at 257 or 200 °C after acid treatment could be ascribed to the removal of partially destructed HMI molecules.

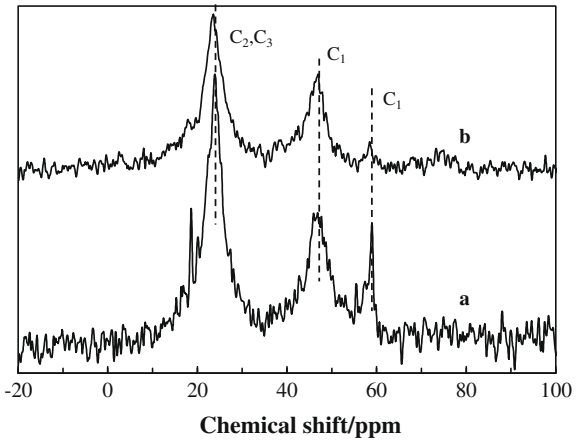

Fig. 15. ^{13}C CP/MAS NMR spectra of (a) hydrothermally synthesized B-MWW-PI and (b) postsynthesized Al-MWW-PI lamellar precursors.

For the postsynthesized Al-MWW-PI lamellar precursor, four weight-loss regions of 150–300, 300–380, 380–470, and 470–700 °C were observed in the range from 150 to 700 °C. In contrast, an obvious weight loss was present solely in the region of 300–400 °C for the acid-treated sample, while a subsequent continuous weight loss of 3.4% occurred below 700 °C. This is consistent with the DTA results of both the samples; upon acid treatment, only one exothermic peak at 348 °C was clearly visible, while the other two exothermic peaks at about 435 and 593 °C drastically decreased in intensity. This shows that most of the PI molecules hard to be oxidized in air could be removed by acid washing, whereas a part of the PI molecules oxidized at low temperature were still occluded in the acid-washed sample. As is shown above, the postsynthesized Al-MWW-PI lamellar precursor could be transformed into Al-YNU-1 through acid treatment, while the Al-MWW-HMI lamellar precursor gave a 3D Al-MWW structure regardless of the synthesis methods, framework Si/Al ratios, and acid treatments. Thus, it could be deduced that the templating molecules oxidized at high temperature might strongly affect the structure, hindering the formation of YNU-1 phase. If T sites in the interlayer void space, including in the supercages, are occupied by Al^{3+} ions, protonated HMI molecules sited between layers would have a strong interaction with zeolite framework, and thus, would be more difficult to be oxidized, compared to free HMI molecules. The existence of interaction between HMI molecules and zeolite framework is supported by the observation that the exothermic peaks at high temperature of the sample postsynthesized from a synthesis gel having a low Si/Al ratio of 20 were much more intense than those of the sample postsynthesized from a gel having a high Si/Al ratio of 140 (Figs. 10 and 13). This is expected since incorporation of more Al^{3+} ions in the framework needs more protonated HMI molecules to compensate the negative charges.

In addition, the HMI molecules hydrogen bonded to defect sites between layers and tightly constrained in the interlayer space would also be hard to be washed away by acid. These and interlayer protonated HMI molecules, particularly those associated with T_1 sites [1] would greatly influence the interlayer structure. If they could not be removed by acid washing, the calcination would allow only a type-A stacking of crystalline layers [29], leading to formation of a 3D MWW structure through the condensation of the silanol groups at T_1 sites (Fig. 16). In contrast, for the postsynthesized Al-MWW-PI lamellar precursor, the PI molecules trapped in the interlayer region cause a random stacking of the layers along *c* axis at a well-defined distance [29]. A nearly complete removal of PI molecules interacted with T sites in the interlayer void space, and in particular, with T_1 sites by the acid treatment would result in the formation of a large number of stacking faults between layers, which might play an important role in the formation of Al-YNU-1 structure [9,10] while it is suggested that this structure was formed through pillaring the crystalline sheets with silicate species [26].

3.4. Catalytic properties of the prepared H-Al-MWW and H-Al-YNU-1

Compared to H-Al-MWW, H-Al-YNU-1 has an expanded pore opening of the 12-membered ring connecting to supercages, while the rigid structure within layers was the same [9,10,26]. Thus, H-Al-YNU-1 would be much more effective than H-Al-MWW for catalyzing the reactions involving bulky molecules. Table 1 summarizes the catalytic results obtained on various zeolites in alkylation of anisole with benzyl alcohol. Evidently, a substantially higher TON was obtained on the H-Al-YNU-1 (284) than on the

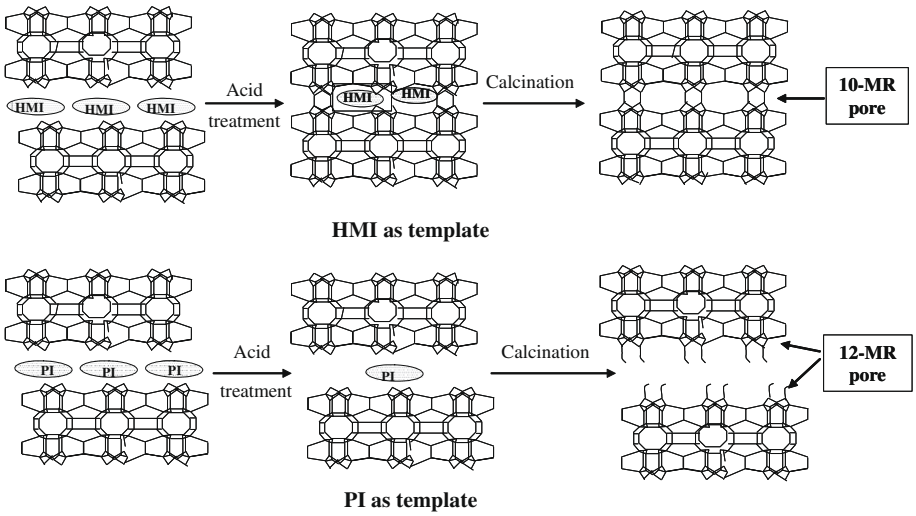

Fig. 16. Structural scheme for the evolution of postsynthesized Al-MWW-HMI and Al-MWW-PI samples during the processes of acid treatment and further calcination.

Table 1
Catalytic results for the alkylation of anisol with benzyl alcohol over different zeolites.[a]

Catalyst	Si/Al	Total acid amount (mmol/g)[b]	Strong acid/weak acid (mmol/mmol)	Conversion (%)	TON based on Al[c]	Selectivity (%)		
						2-Benzyl anisole	4-Benzyl anisole	Ether
H-Al-Beta	12.5	0.46	1.42	51.9	21.0	34.3	46.3	19.3
H-USY	7	0.11	0	74.1	17.8	40.7	52.1	7.2
H-Al-MWW	25	0.41	1.21	71.3	55.6	51.3	38.0	10.7
H-Al-YNU-1	135	0.18	18.5	69.6	284	47.7	39.5	12.8
H-Al-ZSM-5	12.5	1.20	3.42	1.5	0.6	18.7	22.1	59.2
H-Al-MOR	7.5	1.19	7.57	58.2	14.8	40.9	46.3	12.8

[a] *Reaction conditions:* 50 mmol anisole, 5 mmol benzyl alcohol, 0.1 g catalyst, 100 °C, 5 h.
[b] Total acid amounts of various zeolites were calculated by comparing their total NH_3-desorption peak area attributed to both the weak and the strong acid sites with that of H-Al-ZSM-5, respectively. The acid amount of H-Al-ZSM-5 was estimated by assuming that all Al atoms have been incorporated in the framework and one Al produce one acid site [32].
[c] TON was calculated on the basis of Al content in the sample.

other zeolites, showing that H-Al-YNU-1 is the most active catalyst. This could be accounted for by the intrinsic activity of acid sites and the geometric structure of the zeolites. H-USY, H-Al-Beta, and H-Al-MOR all have 12-MR pore openings, which would have no steric effects on the accessibility of reactants to acid sites and on the diffusion of products out of zeolite channels. Thus, a low activity attained on these three types of zeolites was attributed to their acidity, including acid amount, acid strength, and acid type. In contrast, the lower activity obtained on the H-Al-MWW was not only due to its acidity different from that of H-Al-YNU-1 (as shown below) but also attributed to the geometric constraint of its interlayer 10-MR pore openings since this material was synthesized by the same method and had the same intralayer structure as H-Al-YNU-1. Nevertheless, H-Al-MWW showed a much higher benzyl alcohol conversion than H-Al-ZSM-5 did perhaps due to the presence of a lot of side pockets on the external surface and of intrinsically more active acid sites. Because of the intramolecular steric constraint, 2-benzylanisole would be more difficult to form than 4-benzylanisole over zeolite catalysts. However, H-Al-MWW and H-Al-YNU-1 showed higher selectivity of 2-benzylanisole than 4-benzylanisole. This might be accounted for by the unique geometric structure of supercages or side pockets since the 10-MR pore openings of H-Al-MWW would refrain the reactants and particularly the products from diffusing into/out of the channels.

The benefit of the large pore opening of H-Al-YNU-1 was also verified by the catalytic results obtained in the Baeyer–Villiger reaction of cyclohexanone with bulkiness corresponding to 12-MR pore openings; H-Al-YNU-1 gave a cyclohexanone conversion of 44.7%, being double of that obtained on the H-Al-MWW (22.3%) despite that ε-caprolactone as the major product with a certain amount of 6-hydroxycaproic acid and other products were obtained on both the samples (reaction conditions: 0.1 g catalyst, 5 mL acetonitrile, 5 mmol substrate, 5 mmol H_2O_2 (35% in aqueous solution), 75 °C, 2 h).

In the Friedel–Crafts acylation of anisole with acetic anhydride, the highest conversion of 18.0% was also obtained on the H-Al-YNU-1 irrespective of its very low Al content (Table 2). In contrast, no product was detected on the H-USY. H-Al-MOR was nearly inactive, either. As for H-Al-Beta and H-Al-ZSM-5, a moderate conversion was obtained. Both H-Al-MWW and Expanded H-Al-MWW gave a conversion (4.9% and 6.8%, respectively) significantly lower than that attained on the H-Al-YNU-1 although the selectivity of *p*-methoxyacetophenone was higher than 98% for all the samples likely due to the electronic effect of the anisole, the intramolecular steric constraint of *o*-methoxyacetophenone and the electrophilic substitution character of the reaction [31]. This further shows that the geometric structure is not the sole factor that determines the catalytic performance. Zeolite acidity also has a strong influence on their catalytic behavior.

The acidity of various zeolites was investigated by temperature-programed desorption of ammonium (NH_3-TPD) and IR spectroscopy of observed pyridine adsorption. In the NH_3-TPD profile (Fig. 4), H-Al-ZSM-5, H-Al-MWW, H-Al-Beta, and H-Al-MOR showed two desorption peaks, whereas both H-USY and H-Al-

Table 2
Catalytic results for the acylation of anisole with acetic anhydride over various zeolites.[a]

Catalyst	Conversion (%)	TON based on Al[b]	Selectivity (%)	
			p-MAP[c]	*o*-MAP
H-Al-Beta	11.3	4.6	>99	–
H-Al-MOR	0.52	0.1	>99	–
H-USY	0	0	–	–
Expanded H-Al-MWW	6.9	7.4	>9	–
H-Al-YNU-1	18.0	73.4	99.0	1.0
H-Al-MWW	4.3	3.4	>99	–
H-Al-ZSM-5	10.8	4.3	98.6	1.4

[a] Reaction conditions: 0.1 g catalyst, 20 mmol of anisole, 5 mmol of acetic anhydride, 80 °C, 5 min.
[b] TON was calculated on the basis of Al content in the sample.
[c] MAP: methoxyacetophenone.

YNU-1 displayed only one peak around 220 and 326 °C, respectively. The low temperature peak (e.g. <200 °C) is attributed to the desorption of NH_3 adsorbed on the weak acid sites, whereas the high temperature is ascribed to the desorption of NH_3 adsorbed on the strong acid sites [32]. This shows that H-Al-YNU-1 primarily possessed strong acid sites originating from bridging Si–OH–Al groups [18,30]. The total acid amounts and the ratios of the strong acid sites to the weak ones of various zeolites are given in Table 1. It seems that the activity of these zeolites in the Friedel–Crafts acylation of anisole with acetic anhydride was not directly dependent on the acid amount and acid strength, as suggested by the finding that H-Al-MOR with a large amount of quite strong acid sites showed a marginal conversion (Table 2). Nevertheless, it can be found that moderately strong acid sites, corresponding to the NH_3 desorption peaks between 250 and 400 °C, were active for acylation of anisole with acetic anhydride.

Fig. 17 shows the difference IR spectra of pyridine adsorbed on various zeolites. It is clear that all samples had both Brönsted acid sites and Lewis acid sites, as evidenced by the observation of two absorbance bands around 1540 and 1450 cm^{-1} [30]. In the case of H-Al-YNU-1 (Fig. 17A), at least two bands (at 1536 and 1541 cm^{-1}) could be resolved from the broad 1540 cm^{-1} band, whereas three bands could be distinguished from the 1450 cm^{-1} band despite the fact that the two bands at 1439 and 1445 cm^{-1} substantially decreased in intensity with increasing evacuation temperature. This held true for the postsynthesized H-Al-MWW (Fig. 1S) and the Expanded H-Al-MWW (Fig. 17B), and can be accounted for by insertion of Al in crystallographically inequivalent lattice sites [33,34]. Nevertheless, when the evacuation temperature reached 400 °C, the 1450-cm^{-1} band attributed to Lewis acid sites almost disappeared for the H-Al-YNU-1, whereas it was still very distinct in the spectra of the H-Al-MWW and the Expanded H-Al-MWW. This shows that the strong acid sites in the H-Al-YNU-1 are dominantly Brönsted acid sites, while they are consisted of both Lewis acid sites and Brönsted acid sites for the H-Al-MWW and the Expanded H-Al-MWW. The presence of strong Lewis acid sites in the Expanded H-Al-MWW is probably due to substitution of framework Al by Si in the silylation process, leading to formation of a certain amount of octahedral Al species which cannot be removed by acid washing, as substantiated by ^{27}Al MAS NMR spectroscopy (not shown here). As for H-Al-MWW, it may arise from the Al species sited between layers. A part of these Al species could be transformed to octahedral species or tiny Al_2O_3 particles during calcination of the as-synthesized Al-MWW lamellar precursor. This is essentially in agreement with the fact that a large amount of octahedral Ti species and TiO_2 would be present in the sample if the as-synthesized Ti-MWW lamellar precursor was not washed with acid under reflux conditions before calcination [35].

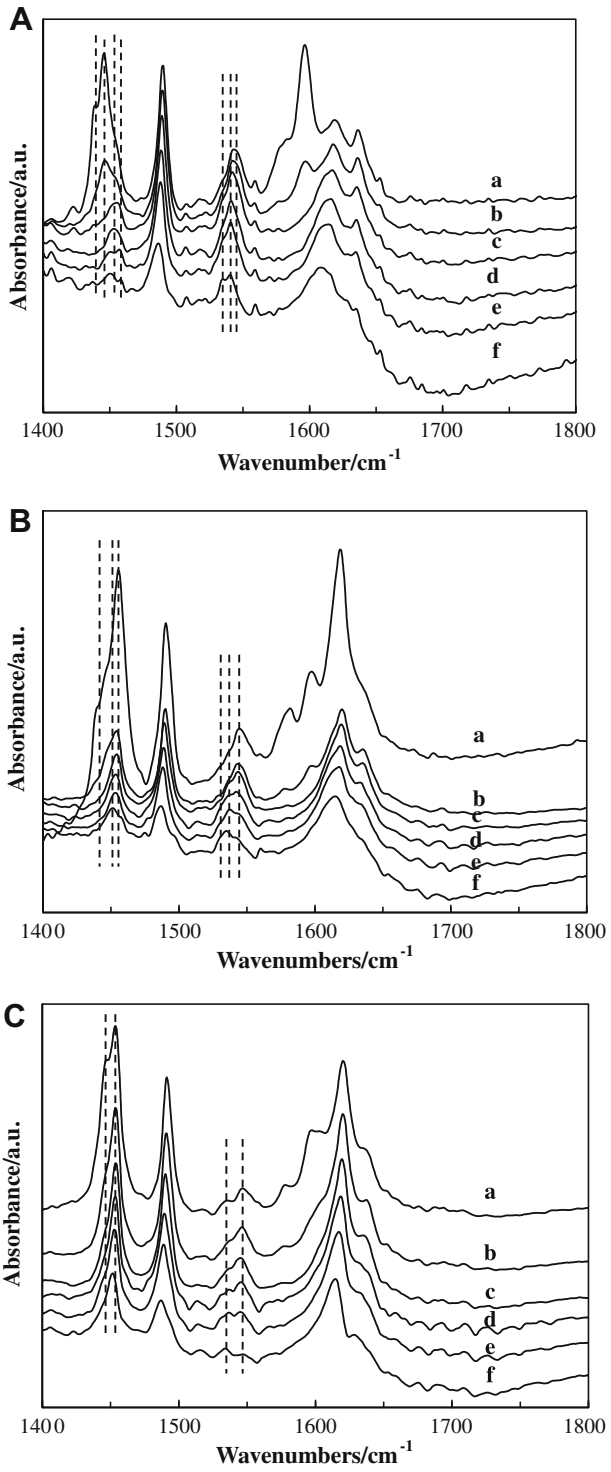

Fig. 17. Differential IR spectra of pyridine adsorbed on (A) H-Al-YNU-1, (B) Expanded H-Al-MWW, and (C) H-Al-Beta at (a) 100 °C, (b) 150 °C, (c) 200 °C, (d) 250 °C, (e) 300 °C, and (f) 400 °C.

With respect to H-Al-MOR, a difference IR spectrum comparable to those of H-Al-MWW and Expanded H-Al-MWW was obtained (Fig. 1S). In contrast, the 1540-cm^{-1} band in the spectrum of H-Al-Beta completely disappeared at 400 °C, while an intense band was still observed at about 1450 cm^{-1} (Fig. 17C). This shows that very strong acid sites in H-Al-Beta are primarily composed of Lewis acid sites, being consistent with the fact that the 1450-cm^{-1} band was much more intense than the 1540-cm^{-1} one irrespective of the

evacuation temperature (Fig. 17C). As expected, both the 1450-cm^{-1} and the 1540-cm^{-1} bands became invisible for H-USY when the evacuation temperature was increased to 400 °C because of its low acid strength (Fig. 1S). Nevertheless, the intensity of the 1450-cm^{-1} band was significantly higher than that of the 1540-cm^{-1} band below 300 °C, showing that Lewis acid sites were predominant in H-USY.

In combination with the NH_3-TPD results, it could be inferred that moderately strong Brönsted acid sites, corresponding to the NH_3 desorption peaks centered between 250 and 400 °C, might act as active centers in the acylation of anisole with acetic anhydride. Neither too strong nor too weak acid sites functioned as active species. Even if the very strong acid sites could catalyze this reaction, the strong adsorption of *p*-methoxyacetophenone and diacetylated and triacetylated anisoles on these acid sites would deactivate the zeolite catalysts quickly by limiting the adsorption of anisole [31,36]. However, we cannot exclude the possibility that a small number of Lewis acid sites might also play an important catalytic role in this reaction.

4. Conclusions

H-Al-MWW with a Si/Al ratio in the range from 10 to ∞ has been synthesized by the postsynthesis method in the presence of hexamethyleneimine. However, the as-synthesized Al-MWW-HMI lamellar precursor could not be transformed into the Al-YNU-1 phase through acid treatment before calcination regardless of the synthesis methods and framework Si/Al ratio. To prepare Al-YNU-1 in a way similar to that adopted for preparing Ti-YNU-1, PI should be used as a templating molecule. It was shown that most of hardly oxidized PI molecules in the postsynthesized Al-MWW-PI precursor could be washed away by acid at boiling temperature, whereas such a type of HMI molecules was still mostly retained in the acid-treated Al-MWW-HMI sample. These hardly oxidized templating molecules may strongly interact with the zeolite framework or be tightly constrained between layers, and thus, markedly affect the structure. An effective removal of these templating molecules by acid treatment would generate a large number of stacking faults, resulting in the formation of YNU-1 structure.

H-Al-YNU-1 exhibited pore properties of 12-MR zeolites. Its pore opening connected to supercages was intermediate between those of H-Al-MOR and H-Al-Beta. It dominantly possessed Brönsted acid sites with moderate strength. As a consequence, it was much more active than H-Al-MWW, H-Al-ZSM-5, H-Al-MOR, H-USY, H-Al-Beta, and Expanded H-Al-MWW for the alkylation of anisole with benzyl alcohol and the acylation of anisole with acetic anhydride. In the Baeyer–Villiger reaction of cyclohexanone with bulkiness corresponding to 12-MR pore openings, H-Al-YNU-1 gave a cyclohexanone conversion double of that obtained on the H-Al-MWW.

Acknowledgments

This work is supported by the National Science Foundation of China (Nos. 20773153 and 20876163), the National Basic Research Program (No. 2009CB226101), and the "Hundred Talents Project" of the Chinese Academy of Sciences. T.T. thanks the support of the Ministry of Education, Culture, Science and Technology of Japan.

Appendix A. Supplementary material

Supplementary data associated with this article can be found, in the online version, at doi:10.1016/j.jcat.2009.06.017.

References

[1] M.E. Leonowicz, J.A. Lawton, S.L. Lawton, M.K. Rubin, Science 264 (1994) 1910.
[2] J.C. Cheng, T.F. Degnan, J.S. Beck, Y.Y. Huang, M. Kalyanaraman, J.A. Kowalski, C.A. Loehr, D.N. Mazzone, Stud. Surf. Sci. Catal. 121 (1999) 53.
[3] A. Corma, V. Gonzàlez-Alfaro, A.V. Orchillès, Appl. Catal. A 129 (1995) 203.
[4] A. Corma, Joaquín Martínez-Triguero, J. Catal. 165 (1997) 102.
[5] C. Ngamcharussrivichai, A. Imyim, X. Li, K. Fujimoto, Ind. Eng. Chem. Res. 46 (2007) 6883.
[6] P. Wu, T. Tatsumi, T. Komatsu, T. Yashima, J. Catal. 202 (2001) 245.
[7] W. Fan, P. Wu, T. Tatsumi, J. Catal. 256 (2008) 62.
[8] A. Corma, V. Fornes, S.B. Pergher, Th.L.M. Maesen, J.G. Buglass, Nature 396 (1998) 353.
[9] W. Fan, P. Wu, S. Namba, T. Tatsumi, Angew. Chem., Ed. Int. 43 (2004) 236.
[10] W. Fan, P. Wu, S. Namba, T. Tatsumi, J. Catal. 243 (2006) 183.
[11] R. Aiello, F. Crea, F. Testa, G. Demortier, P. Lentz, M. Wiame, J.B. Nagy, Micropor. Mesopor. Mater. 35–36 (2000) 585.
[12] J. Güray, J. Warzywoda, N. Baç, A. Sacco Jr., Micropor. Mesopor. Mater. 31 (1999) 241.
[13] When the Si/Al ratio in the synthesis gel was increased to 50, a substantial amount of impurity material of Nonasil was crystallized in the Na_2O–SiO_2–Al_2O_3–HMI-F–H_2O system. A further increase in the Si/Al ratio in the synthesis gel to 100 led to the formation of pure Nonasil phase.
[14] M. Cheng, D. Tan, X. Liu, X. Han, X. Bao, L. Lin, Micropor. Mesopor. Mater. 42 (2001) 307.
[15] J. Plévert, K. Yamamoto, G. Chiari, T. Tatsumi, J. Phys. Chem. B 103 (1999) 8647.
[16] J. Xia, D. Mao, W. Tao, Q. Chen, Y. Zhang, Y. Tang, Micropor. Mesopor. Mater. 91 (2006) 33.
[17] M.A. Asensi, A. Corma, A. Martínez, J. Catal. 158 (1996) 561.
[18] L. Liu, M. Cheng, D. Ma, G. Hu, X. Pan, X. Bao, Micropor. Mesopor. Mater. 94 (2006) 304.
[19] P. Wu, J. Ruan, L. Wang, L. Wu, Y. Wang, Y. Liu, W. Fan, M. He, O. Terasaki, T. Tatsumi, J. Am. Chem. Soc. 130 (2008) 8178.
[20] S. Inagaki, T. Tatsumi, Chem. Commun. (2009) 2583.
[21] After repeatedly ion-exchanging Na^+ with NH_4^+ (0.5 mol/L NH_4NO_3, 70 °C, 3 h) for 3 times, the interlayer structure of Expanded Na-Al-YNU-1 was significantly deteriorated, being nearly recovered to that of Al-MWW.
[22] P. Wu, T. Tatsumi, Chem. Commun. (2002) 1026.
[23] M.M.J. Treacy, J.B. Higgins, Collection of Simulated XRD Patterns for Zeolites, fifth revised ed., Elsevier, 2007. p. 302.
[24] W. Kolodziejski, C. Zicovich-Wilson, C. Corell, J. Pérez-Pariente, A. Corma, J. Phys. Chem. 99 (1995) 7002.
[25] D. Nuntasri, P. Wu, T. Tatsumi, J. Catal. 213 (2003) 272.
[26] J. Ruan, P. Wu, B. Slater, O. Terasaki, Angew. Chem., Int. Ed. 44 (2005) 6719.
[27] S.L. Lawton, A.S. Fung, G.J. Kennedy, L.B. Alemany, C.D. Chang, G.H. Hatzikos, D.N. Lissy, M.K. Rubin, H.C. Timken, S. Steuernagel, D.E. Woessner, J. Phys. Chem. 100 (1996) 3788.
[28] G.J. Kennedy, S.L. Lawton, A.S. Fung, M.K. Rubin, S. Steuernagel, Catal. Today 49 (1999) 385.
[29] R. Millini, G. Perego, W.O. Parker Jr., G. Bellussi, L. Carluccio, Micropor. Mater. 4 (1995) 221.
[30] H.G. Karge, E. Geidel, in: H.G. Karge, J. Weitkamp (Eds.), Molecular Sieves Science and Technology, vol. 4, Springer, 2004, p. 131.
[31] M. Guidotti, C. Canaff, J. Coustard, P. Magnoux, M. Guisnet, J. Catal. 230 (2005) 375.
[32] N. Katada, M. Niwa, Catal. Surv. Asia 8 (2004) 161.
[33] B. Onida, F. Geobaldo, F. Testa, F. Crea, E. Garrone, Micropor. Mesopor. Mater. 30 (1999) 119.
[34] M. Bevilacqua, D. Meloni, F. Sini, R. Monaci, T. Montanari, G. Busca, J. Phys. Chem. C 112 (2008) 9023.
[35] P. Wu, T. Tatsumi, T. Komatsu, T. Yashima, Chem. Lett. (2000) 774.
[36] D. Rohan, C. Canaff, E. Fromentin, M. Guisnet, J. Catal. 177 (1998) 296.